ACS Catalysis

Research Article

pubs.acs.org/acscatalysis

Mechanistic Studies on the Alkylation of Amines with Alcohols Catalyzed by a Bifunctional Iridium Complex

Agnieszka Bartoszewicz,[†,‡,⊥] Greco González Miera,[†,‡,⊥] Rocío Marcos,[†,‡,⊥] Per-Ola Norrby,[§,∥] and Belén Martín-Matute*[,†,‡]

[†]Organic Chemistry Department, Arrhenius Laboratory, and [‡]Berzelii Center EXSELENT on Porous Materials, Stockholm University, SE-106 91 Stockholm, Sweden

[§]Chemistry and Molecular Biology Department, Gothenburg University, Kemigården 4, SE-412 96 Gothenburg, Sweden

[∥]Pharmaceutical Development, AstraZeneca, Pepparedsleden 1, SE-431 83 Mölndal, Sweden

Supporting Information

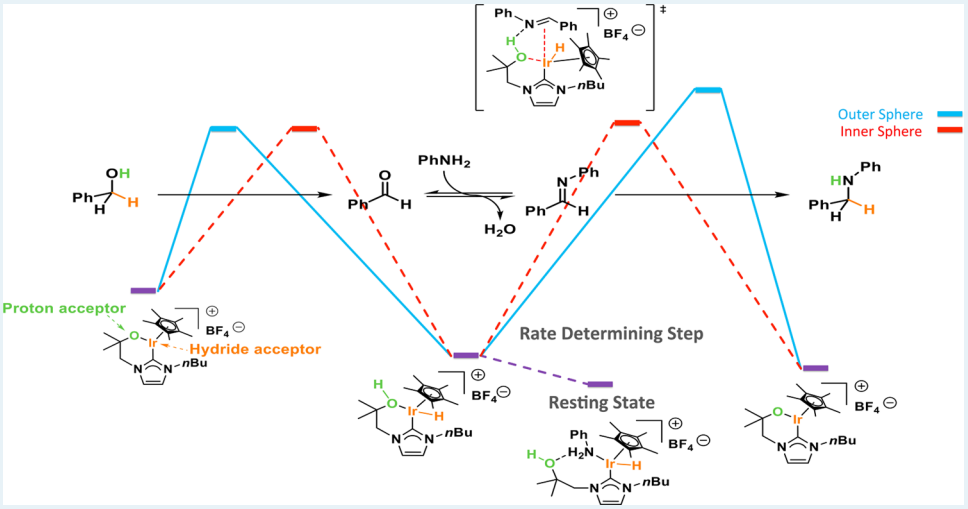

ABSTRACT: The mechanism of the N-alkylation of amines with alcohols catalyzed by an iridium complex containing an N-heterocyclic carbene (NHC) ligand with a tethered alcohol/alkoxide functionality was investigated by a combination of experimental and computational methods. The catalyst resting state is an iridium−hydride species containing the amine substrate as a ligand, and decoordination of the amine, followed by coordination of the imine intermediate to the iridium center, constitute the rate-determining step (rds) of the catalytic process. The alcohol/alkoxide that is tethered to the NHC participates in every step of the catalytic cycle by accepting or releasing protons and forming hydrogen bonds with the reacting species. Thus, the iridium complex with the alcohol/alkoxide tethered to the N-heterocyclic carbene ligand acts as a bifunctional catalyst.

KEYWORDS: *iridium, amine alkylation, Hammett plots, kinetics, DFT calculations*

INTRODUCTION

The condensation of alcohols with amines catalyzed by transition-metal complexes[1] has, in the past decade, been shown to be a very powerful method for synthesizing N-substituted amines.[2] The transformation is highly atom economical and environmentally friendly, since water is produced as the sole byproduct. Moreover, alcohols, the substrates for the reaction, are readily available in great numbers and variety. Successful examples have been reported using complexes of Ir, Ru, Pd, and Fe among others.[3−12]

We have reported the synthesis of an iridium complex (**1**) that features an N-heterocyclic carbene (NHC) ligand functionalized with an additional coordinating group, a tertiary alcohol.[12] Complex **1** showed remarkably high activity in the alkylation of amines with alcohols under base-free and relatively mild reaction conditions (Scheme 1). This is the first complex with an aliphatic alcohol functionalized bidentate ligand that has been successfully used in hydrogen-transfer reactions; the majority of complexes used in such reactions have relied on amine/amido[13,14] and phenol/carbonyl moieties as the donor groups.[15−17] Importantly, to the best of our knowledge, the metal−ligand bifunctionality of such systems containing a tertiary alcohol[18] group has not yet been demonstrated.

Received: March 26, 2015
Revised: May 4, 2015
Published: May 5, 2015

DOI: 10.1021/acscatal.5b00645
ACS Catal. 2015, 5, 3704−3716

Scheme 1. Alkylation of Amines with Alcohols Catalyzed by Complex 1

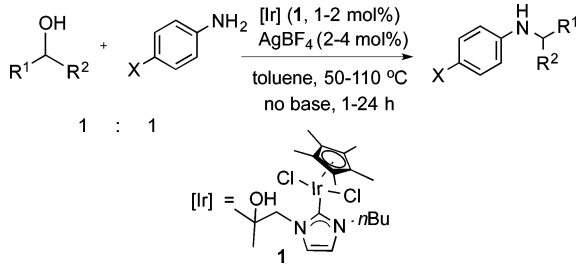

The mechanism of the alkylation of amines with alcohols has been studied both experimentally and computationally for some catalytic systems, with the following common general steps:[7c,19,20] (i) oxidation (dehydrogenation) of the alcohol substrate to form an aldehyde,[21] (ii) condensation of the aldehyde with the amine substrate to give an imine intermediate, and (iii) reduction of the imine. The catalyst oscillates between two forms: dehydrogenated and hydrogenated. Metal complexes that are used in well-established hydrogen-transfer processes (e.g., the reduction of ketones using isopropyl alcohol as the hydrogen donor) have also shown good activity in the alkylation of amines with alcohols.[22] This is to be expected, since the key mechanistic steps of the two reactions are conceptually related.[23] The extensive mechanistic investigations that have been carried out on transfer hydrogenation reactions give very relevant insights into the mechanism of the alkylation of amines with alcohols.[24]

Two reports by Eisenstein and Crabtree[20] and by Madsen and Fristrup[7d] addressed the details of the catalytic cycle in the reaction catalyzed by iridium complexes. In both studies, the mechanism of the reaction catalyzed by $[Cp^{(*)}IrCl_2]_2$ was investigated using a combination of experimental and theoretical approaches. The key intermediates proposed in the two papers are different. Eisenstein, Crabtree, and co-workers pointed out the important role of the carbonate additive, which can act as a participating ligand, and proposed $[CpIr(CO_3)]$ (**2**) to be the active catalyst (Scheme 2a).[20] On the other hand, Madsen, Fristrup, and co-workers suggested that a complex formed upon coordination of the amine substrate, $[Cp^*Ir(NH_2Ph)X]^+$ (**3**), is the key catalytic species (Scheme 2a).[7c] The conclusions of these reports differ in a number of important aspects, including the identity of the rate-determining step (rds).

Scheme 2. Presumed Active Species Generated in the N-Alkylation of Amines with Alcohols: (a) Proposals by Eisenstein and Crabtree and by Fristrup and Madsen; (b) This Work

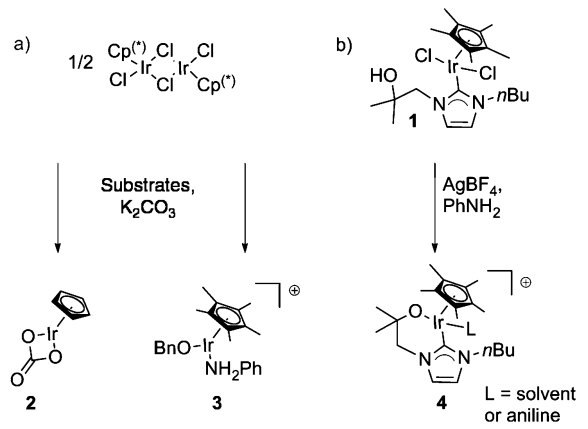

In this paper, we present detailed experimental and theoretical mechanistic studies on the N-alkylation of amines with alcohols catalyzed by iridium complex **1** (Scheme 1). We have investigated the existence of a cooperative interaction of the metal center and the ligand in this catalytic system and have identified the rds of the reaction. Various experimental techniques, such as reaction-order studies, kinetic isotope effect measurements, and Hammett studies, gave information about the structure of the active catalyst, as well as the relative rates of the individual mechanistic steps. Theoretical investigations allowed the elucidation of the fine details of the catalytic cycle.

A number of interesting features of the mechanism that distinguish it from those studied before were discovered. In particular, it was found that the resting state of the catalyst consists of an iridium−hydride species coordinated to the amine substrate and also that imine coordination is the rds. The theoretical studies presented here show that the tertiary alcohol/alkoxide moiety of the ligand plays an important role in the catalytic cycle and can be considered a novel type of functional group in metal−ligand bifunctional systems.

RESULTS AND DISCUSSION

Experimental Investigations. *Reaction Order.* We began our investigations by determining the order of reaction for each of the reactants (benzyl alcohol **5a** and aniline **6a**), for the products (**7a** and H_2O), and for the catalyst (**1**) in the reaction shown in Scheme 3, using the method of initial rates.

Scheme 3. Model Reaction for Experimental Investigation of Reaction Orders

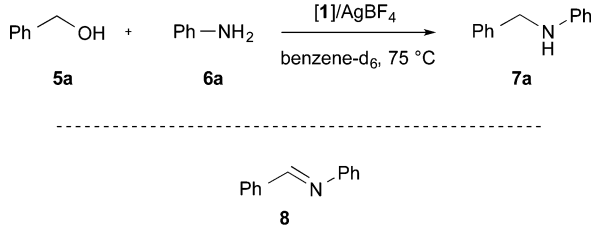

Additionally, the influence of the putative imine intermediate (benzylidenaniline **8**) on the rate was also investigated. All reactions were carried out in benzene-d_6 at 75 °C and monitored by ^{1}H NMR spectroscopy.

We found that the initial rate is not influenced by the concentration of benzyl alcohol (**5a**; Figure 1), but it is inversely proportional to the concentration of aniline (**6a**; Figure 2). The fact that the rate is independent of the concentration of **5a** suggests that the dehydrogenation step cannot be the rds of the catalytic cycle. On the other hand, the inhibition of the reaction by **6a** indicates the existence of a resting state where **6a** acts as a ligand. Regarding the products of the reaction, it was established that the concentration of **7a** does not affect the initial rate (see Figure S4 in the Supporting Information). As shown in Figure 3, the initial rate is inversely proportional to the concentration of water. Since it is unlikely that water is a good ligand for iridium (or is at least a better ligand than the amines present in the reaction mixture), its inhibitory effect may be ascribed to a shifting backward of the

DOI: 10.1021/acscatal.5b00645
ACS Catal. 2015, 5, 3704−3716

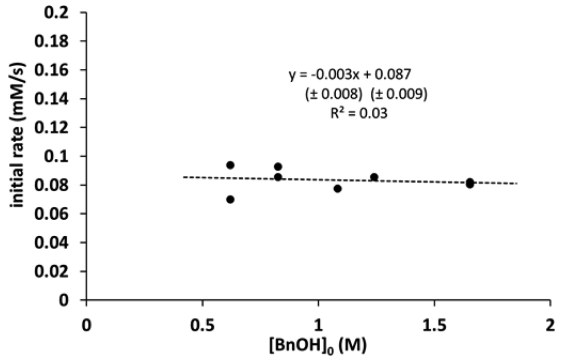

Figure 1. Dependence of the initial rate on benzyl alcohol (**5a**) concentration.

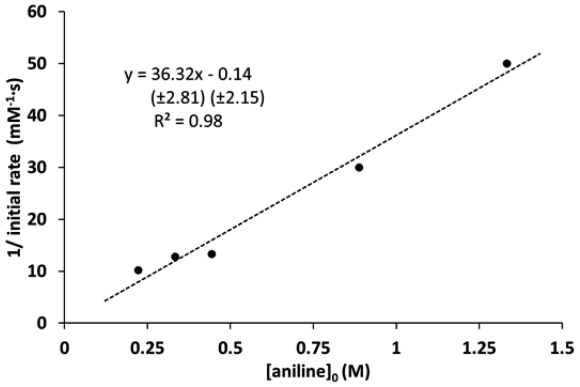

Figure 2. Dependence of the reciprocal initial rate on aniline (**6a**) concentration.

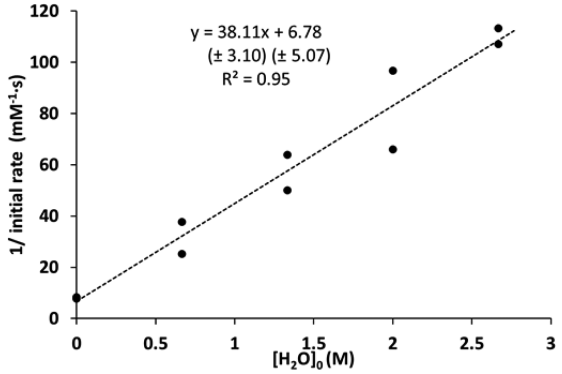

Figure 3. Dependence of the reciprocal initial rate on water concentration.

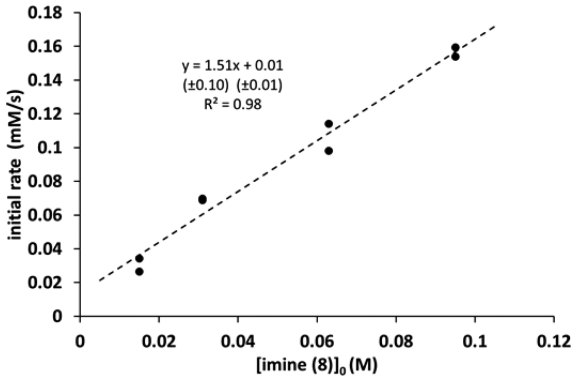

Figure 4. Dependence of the initial rate on imine (**8**) concentration.

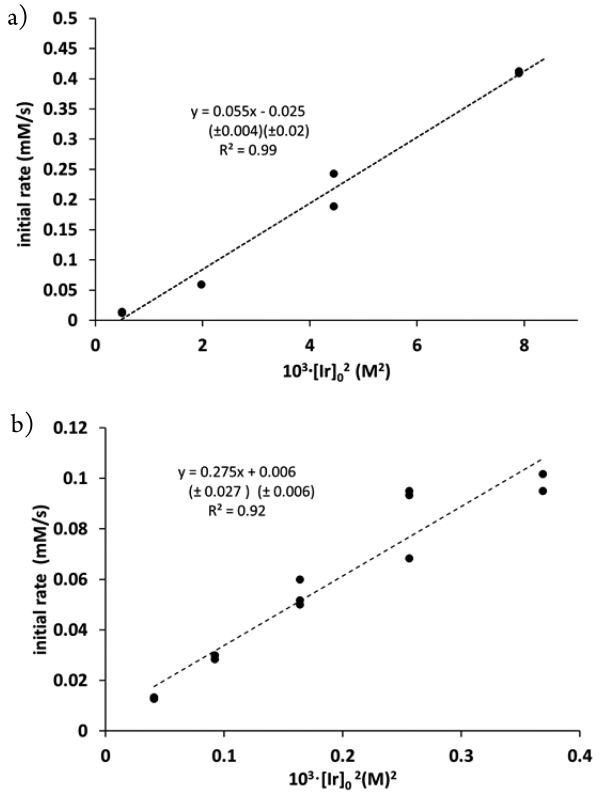

Figure 5. (a) Dependence of the initial rate on the square of catalyst concentration. (b) Dependence of the initial rate on the square of catalyst concentration in experiments with 15 mol % of imine **8**.

equilibrium of imine **8** formation. This in turn implies that the imine intermediate **8** may be involved in the rds. To verify this, we evaluated whether the addition of **8** to the reaction mixture would have an impact on the initial reaction rate. Indeed, it was found that the reaction is first order in imine **8** (Figure 4).

Finally, the reaction was found to have a higher order in catalyst than expected: at least 2 (Figure 5a and Figure S7b–d in the Supporting Information). We cannot fully explain this but can advance a number of possible explanations for the discrepancy. Our plots are based on total amount of added catalyst; the actual concentration of active catalyst could be lower: for example, due to the presence of some unknown inhibitor. Alternatively, the catalyst could have secondary effects, such as changing the pH of the reaction medium, which in turn could affect the reaction rate. Alternatively, if we assume that the alcohol dehydrogenation and the imine formation are both rapid processes, the reaction rate will be controlled by the bimolecular reaction between **8** and iridium hydride species. The concentrations of both of these are proportional to the initial concentration of the catalyst, which could explain the observed high reaction order in catalyst. We therefore investigated the catalyst reaction order in the presence of 15 mol % of imine **8**, which indeed reduced the apparent reaction order in catalyst significantly (Figure 5b and Figures S7b–d in the Supporting Information). We cannot rule out any of these or other similar hypotheses, but we can state that addition of imine lowers the apparent reaction rate in catalyst.

In summary, the reaction-order studies indicate that the rds of the overall transformation lies in the last part of the

DOI: 10.1021/acscatal.5b00645
ACS Catal. 2015, 5, 3704–3716

mechanism (i.e., imine reduction, step iii; vide supra). Furthermore, a complex formed by coordination of aniline to an iridium−hydride species seems to be a likely resting state of the catalyst on the basis of the observed inhibition by aniline.[43]

In Situ Characterization of the Catalyst Resting State. In an attempt to characterize the postulated resting state, the reaction between benzyl alcohol (**5a**) and aniline (**6a**) catalyzed by iridium (**1**/$AgBF_4$, 2 mol %) was monitored by ^{1}H NMR spectroscopy (Figure 6 and Figure S8 in the Supporting

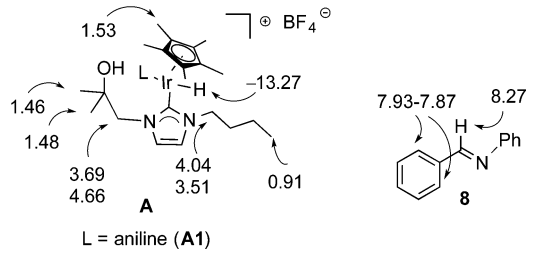

Figure 6. Selected ^{1}H NMR chemical shifts (in ppm) of Ir−hydride resting state **A1** and imine **8** observed in the catalytic reactions.

Information). In addition to the signals originating from the substrates and products, we could observe the imine intermediate **8**. Furthermore, an additional clear signal at high field (−13.27 ppm) indicated the presence of an iridium−hydride species. By integration of the resonances, it was established that the concentration of **8** was comparable to that of the hydride species and that both corresponded well with the initial catalyst concentration (i.e., 2 mol %). The results of the kinetic studies, along with the observation of the Ir−hydride complex, suggest that the resting state of the catalyst is an iridium−hydride complex with aniline coordinated (**A1**) (see Figure 6 for characteristic shifts).

Kinetic Isotope Effect (KIE) Investigations. Kinetic experiments with deuterium-labeled benzylic alcohols were carried out to investigate the relative rates of the alcohol oxidation and imine reduction steps. The progress of the reactions between benzyl alcohol (**5a**) or α-d_2-benzyl alcohol (**5a**-d_2) and aniline (**6a**) was followed by NMR spectroscopy. The decay of the concentration with time was similar for the two substrates (**5a** and **5a**-d_2) (Figure S9 in the Supporting Information), and the calculated KIE was 1.24 ± 0.35.[25] This low KIE value suggests that the alcohol oxidation step is not the rds of the reaction.[26,27]

During the reduction of **8** by the iridium−hydride, an Ir−H bond is broken. Although the KIE resulting from this step should be of a smaller magnitude than that of a KIE due to the cleavage of a C−H bond (the Ir−H bond has a lower force constant), the low KIE determined for the overall reaction is somewhat surprising. It indicates that the breaking of neither the C−H bond nor the Ir−H bond is involved in the rds.

From the kinetic studies on the reaction orders (Figures 1−5), we had concluded that imine **8** and iridium hydride **A** react in the rds. Together with the small KIE measured, it seems reasonable to propose that coordination of the imine to the hydride complex, rather than the subsequent imine reduction step, constitutes the rds. Hammett investigations and theoretical studies (vide infra) will reinforce this conclusion.

To test whether formation of imine **8** takes place within the coordination sphere of iridium, we carried out a crossover experiment (Scheme 4). Thus, a 1:1 mixture of **5a** and **5a**-d_2 was subjected to the reaction with **6a**. The progress of the

Scheme 4. Crossover Experiment

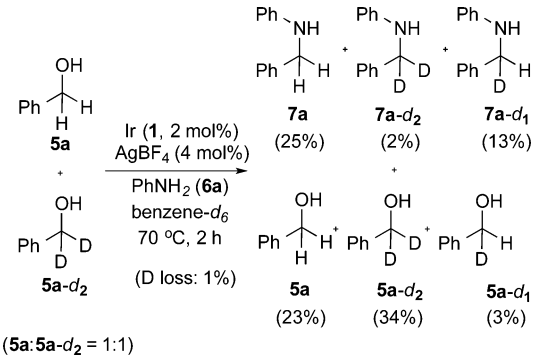

reaction was monitored by ^{1}H and quantitative ^{13}C NMR spectroscopy (Scheme S1 and Figure S10 in the Supporting Information) until approximately 80% conversion was reached (at higher conversions, increased loss of deuterium was observed[25]). The formation of **7a**-d_1 (for example, 13% after 2 h) implies that at least some portion of the intermediate aldehyde (**9a**, **9a**-d_1) produced in the dehydrogenation step leaves the coordination sphere of the iridium hydride/deuteride intermediate. This is because, after condensation of the aldehyde with aniline in solution, the resulting imine may be hydrogenated by an iridium−hydride species containing a different isotope of hydrogen, thus leading to the monodeuterated product **7**-d_1. The formation of a small amount (3%) of monodeuterated benzyl alcohol **5a**-d_1 was also observed. This shows that the alcohol oxidation is effectively almost irreversible.

We also observed that **5a** was consumed more quickly than **5a**-d_2 under competition conditions. The KIE obtained for the alcohol dehydrogenation step was 2.42 ± 0.07 (Figure 7).[26]

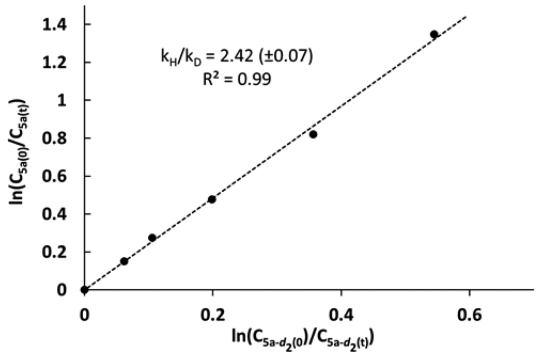

Figure 7. $\ln([C_{5a\text{-}d_2(0)}]/[C_{5a\text{-}d_2(t)}])$ vs $\ln([C_{5a(0)}]/[C_{5a(t)}])$ dependence (0−3 h) in a crossover experiment; $[C_{5a\text{-}d_2(0)}]$ is the initial concentration, and $[C_{5a\text{-}d_2(t)}]$ is the concentration of α-d_2-benzyl alcohol at a given time; $[C_{5a(0)}]$ is the initial concentration, and $[C_{5a(t)}]$ is the concentration of benzyl alcohol at a given time.

This competition KIE together with the low KIE (1.24 ± 0.35) measured from initial rates of two parallel reactions is a clear indication that the alcohol oxidation is not rate limiting and occurs before formation of the resting state.[26]

*Reaction of Enantiopure Phenylethanol ((R)-**10**) with p-Chloroaniline (**6b**).* When (*R*)-1-phenylethanol ((*R*)-**10**, >99% *ee*) was used (Scheme 5 and Figure 8), it underwent only slow racemization under the reaction conditions (77% ee at 85% conversion). This shows that ketones as well as aldehydes

DOI: 10.1021/acscatal.5b00645
ACS Catal. 2015, 5, 3704−3716

Scheme 5. Reaction of an Enantiopure Alcohol

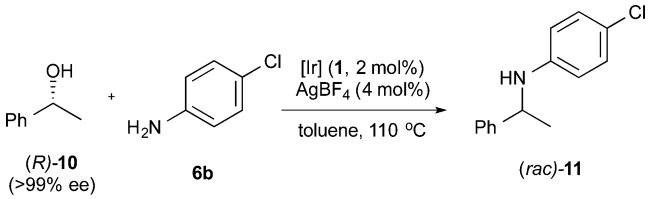

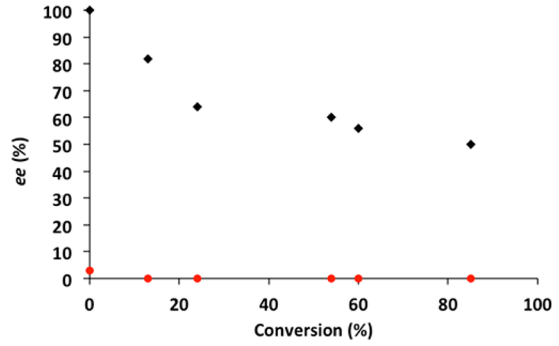

Figure 8. Slow racemization of (*R*)-10 (black ◆) and lack of stereospecificity in the formation of **11** (red ●).

prefer the forward reaction to imine and further reduction over back-reaction between the carbonyl and the iridium−hydride. Interestingly, the product of this reaction (**11**) was formed as a racemate, indicating that the iridium hydride intermediate, which is formally chiral at iridium, racemizes efficiently. An alternative rationalization would be that the chirality transfer from alcohol to iridium and further on to imine is so inefficient that no enantiomeric excess can be detected in the final product.

Hammett Studies. Hammett studies were carried out to obtain additional insights into the mechanism of the reaction.[28] The electronic influence of the para substituents on the alcohol and aniline substrates was investigated using "one-pot" competition experiments[29,30] and noncompetition experiments.

The ρ values obtained in the Hammett competition experiments correspond to the magnitude of charge (positive or negative) that is built up in the transition state in the first irreversible step of the mechanism that involves the substrate under investigation. Thus, these *Hammett studies* conducted using *competition* experiments give information about the step in which selectivity between the competing substrates is decided and not about the overall rds of the mechanism. On the other hand, in the separate experiments ρ is related to the change of charge on the transition states involving the studied substrates during the rds.

Hammett Studies with Anilines. First, we performed Hammett studies under competition conditions with a series of para-substituted anilines (Scheme 6). Assuming that equilibration of the different imines is much faster than the subsequent hydrogenation, i.e., Curtin−Hammett conditions,[31] the experiment should reveal the selectivity-determining step during the imine hydrogenation. A linear plot of $[\log(k_X/k_H)]$ vs neutral ρ value was obtained with a good correlation (Figure 9a and Figures S11 and S13 in the Supporting Information). The negative reaction constant (ρ) indicates that positive charge is built up in the imine moiety in the selectivity-determining transition state. This agrees with imine coordination to the iridium−hydride being an irreversible step and is

Scheme 6. Reaction Conditions Used in the One-Pot Hammett Competition Study of Para-Substituted Anilines

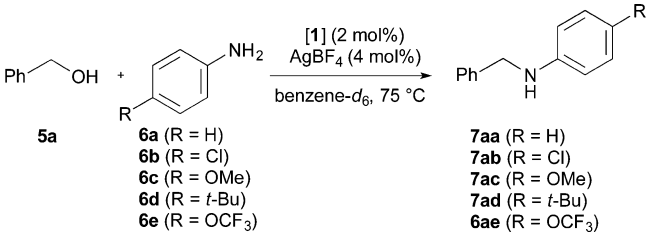

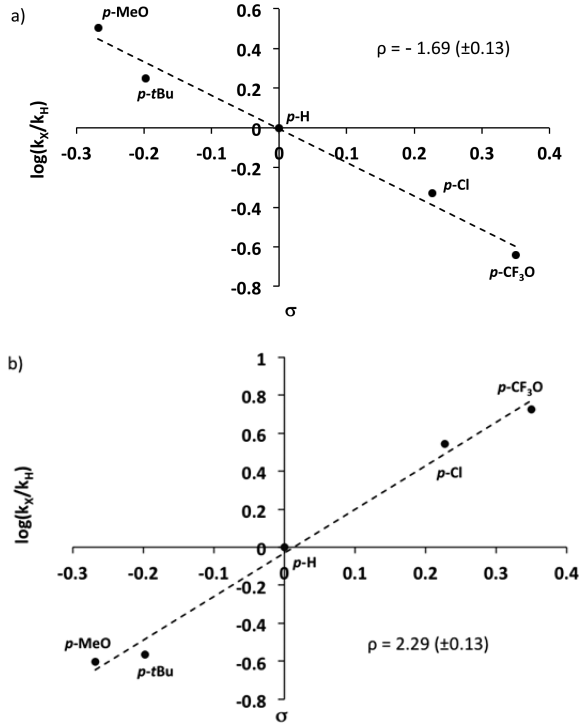

Figure 9. (a) Hammett plot constructed from the relative rates in competition experiments with para-substituted anilines **6a−e** and benzyl alcohol **5a** ($y = -1.69x$ (±0.13) − 0.01 (±0.03); $R^2 = 0.98$). (b) Hammett plot constructed from the relative rates obtained from noncompetition experiments with para-substituted anilines **6a−e** and benzyl alcohol **5a** ($y = 2.29x$ (±0.13) − 0.03 (±0.03), $R^2 = 0.99$).

consistent with the result of KIE studies described in the previous section.

Interestingly, the relative reactivity of the anilines in separate experiments were opposite (Figure 9b and Figure S20 in the Supporting Information) to those observed in the competition experiment. In the former, electron-poor anilines reacted more quickly than electron-rich anilines. These experiments both measure the same step of the mechanism, i.e. coordination of imine **8** to the iridium−hydride intermediate (Figure 6), which consists of dissociation of aniline from **A1** (L = aniline) and subsequent reaction of the resulting complex with **8**. This step is the rds of the overall reaction, and as such, it determines the rates of the separate experiments with different anilines (Figure 9b). On the other hand, it is also the selectivity-determining step for the Hammett competition experiment with anilines.[26] This discrepancy in the relative reactivities of different anilines under competition and noncompetition conditions can be justified. In the noncompetition experiments, both the ground states (Ir−H complexes with the corresponding aniline

DOI: 10.1021/acscatal.5b00645
ACS Catal. 2015, 5, 3704−3716

substrate coordinated) and the transition states (imine coordination) vary and, apparently, the different energies in the ground states have a larger influence on the reaction rate (in other words, the inhibitory power of electron rich anilines outcompetes their high inherent reactivity; Scheme S4 in the Supporting Information). Thus, the reactions involving better-coordinating, electron-rich anilines are slower under non-competition conditions. However, in the competition experiment, there is a common ground state for all of the reactions, the iridium−hydride complex with the most electron rich aniline coordinated, and thus only the transition-state energies for the coordination of the various imines differ. Hence, in this case, the imines derived from the electron-rich anilines react more quickly.

Hammett Studies with Benzyl Alcohols. In the second Hammett competition study, the relative reactivities of several para-substituted benzyl alcohols **5a−d,f** were compared. Since in this experiment the para-substituted aryl moieties originally in the alcohol substrates are present throughout the mechanistic cycle, this study will give information about both alcohol oxidation and imine coordination/reduction. Both of these steps could contribute to the selectivity of the reaction. To determine which of the steps has a dominant influence on the selectivity, three competition experiments were carried out. In each experiment, the same set of alcohols **5a−d,f** was reacted with a different aniline (**6a,c,f**; Scheme 7). Hammett plots with

Scheme 7. Reaction Conditions Used in Three One-Pot Hammett Competition Studies of Para-Substituted Benzyl Alcohols

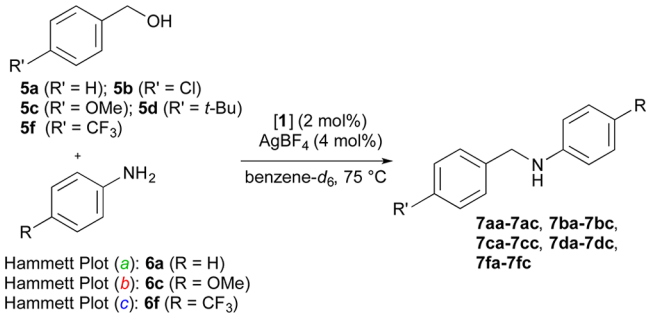

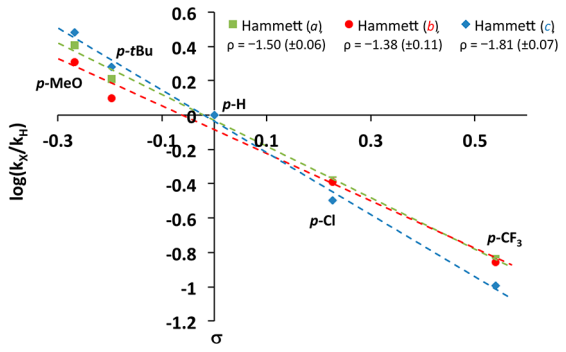

Figure 10. Plots of the Hammett competition studies of the reactions between a set of para-substituted benzyl alcohols (**5a−5d,f**) with three different anilines: $PhNH_2$ (**6a**, Hammett plot *a*; $y = -1.50x$ (±0.06) − 0.03 (±0.02), $R^2 = 0.99$), *p*-$MeOC_6H_4NH_2$ (**6c**, Hammett plot *b*; $y = -1.38x$ (±0.11) − 0.08 (±0.03); $R^2 = 0.98$), and *p*-$CF_3C_6H_4NH_2$ (**6f**, Hammett plot *c*; $y = -1.81x$ (±0.08) − 0.04 (±0.08), $R^2 = 0.99$).

negative ρ values (Figure 10 and Figures S32 and S34 in the Supporting Information) were obtained, indicating that a positive charge is built up at the benzylic carbon in the selectivity-determining transition state. This is consistent with the alcohol oxidation being the first effectively irreversible step, which is in agreement with the KIE investigations (vide supra). No significant differences among the slopes of the three independent Hammett plots were observed, indicating that the alcohol oxidation is likely to be the dominant selectivity-determining step. The ρ value obtained in the experiment with *p*-CF_3-aniline (**6f**) is, however, slightly more negative than those obtained for *p*-OMe-aniline (**6c**) and for aniline (**6a**).

This suggests that in those cases in which electron-poor imines are formed as intermediates, and thus the imine reduction is slower, the alcohol oxidation becomes slightly more reversible and the imine reduction step also contributes to the selectivity of the reaction. Thus, the product-determining step will be highly dependent on the electronic properties of the alcohol and amine substrates and may differ for different reactants.

The trend in the relative reactivity of electronically different benzyl alcohols determined in noncompetition experiments (Figure S21 in the Supporting Information) was found to be the same as that observed in the competition experiments (Figure 10): the reactions proceeded more quickly for electron-rich alcohols than for electron-poor ones. This result is consistent with the imine coordination step being the slowest step in the reaction.

Summary of the Experimental Mechanistic Studies. On the basis of the results of the experiments described above, we propose a plausible reaction mechanism (Scheme 8). In the first step (step *i*) of the catalytic cycle, benzyl alcohol (**5a**) is oxidized to give benzaldehyde (**9a**) and an iridium−hydride complex (**A**). The alcohol oxidation was found to be practically irreversible. After dissociation of aldehyde **9a**, aniline (**6a**) coordinates to the iridium−hydride complex **A** to give hydridic complex **A1** (step *iii*), the resting state of the catalyst. In an

Scheme 8. Summary of Experimental Mechanistic Investigations

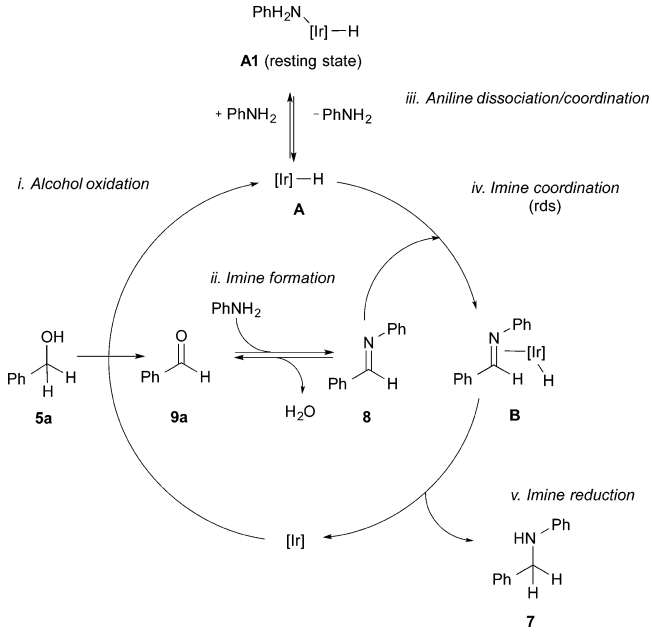

DOI: 10.1021/acscatal.5b00645
ACS Catal. 2015, 5, 3704−3716

independent reaction (step *ii*), **9a** reacts with aniline (**6a**) to give imine **8** and water. The inhibiting effect of water on the reaction rate suggests that the imine formation is a reversible process under the reaction conditions. The next step consists of two substeps: namely dissociation of aniline **6a** from the iridium−hydride complex **A1** and subsequent coordination of imine **8** (step *iv*) to give imine−iridium complex **B**. KIE studies, as well as Hammett investigations, provide evidence that coordination of imine is the rds. After effectively irreversible formation of complex **B**, imine reduction takes place. The *sec*-amine **7** produced as the product of this process does not inhibit the reaction: i.e., it does not form strong complexes with iridium at any stage of the catalytic cycle. The overall proposed catalytic cycle yields a rate law that is consistent with the results of all the experimental mechanistic studies described in the previous sections (see the Supporting Information for details).

Theoretical Investigations. Density functional theory (DFT) calculations were used to study the fine details of the catalytic cycle and to investigate whether the alkoxide/alcohol functional group in the carbene ligand plays an active role in the mechanism: i.e., whether complex **1** works as a metal−ligand bifunctional catalyst. Additionally, we aimed to investigate whether the mechanism follows an inner- or an outer-sphere pathway.

Alcohol Oxidation. On the basis of our earlier experimental results,[12] the cationic iridium complex **INT-1** (Figure 11),

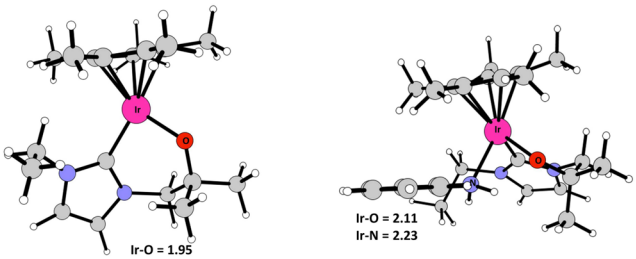

INT-1 (0 kJ/mol) **INT-1A** (−19 kJ/mol)

Figure 11. Optimized structures of an iridium−alkoxide active species (**INT-1**) and of a related complex formed upon coordination of aniline (**INT-1A**). Distances are given in Å.

containing a Cp* ligand and a bidentate carbene ligand functionalized with an alkoxide moiety, was chosen to be the starting point of the catalytic cycle. For the computational studies, the structure of the carbene ligand was simplified by replacing the butyl group with an ethyl substituent. No further simplifications of the catalyst structure were introduced. The free energy profiles were calculated for benzyl alcohol and aniline as model substrates.

The Ir−O distance in **INT-1** is calculated to be only 1.95 Å, which suggests that there is a significant π donation from the alkoxide group to the electron-poor metal center[32] (see Figures 11, 13, 14, and 16 for optimized structures of this and other key intermediates and transition states; the calculated structures of the other stationary points can be found in the Supporting Information). Coordination of aniline (**6a**) to **INT-1** results in the formation of **INT-1A**, which is more stable than **INT-1** by 19 kJ/mol (Figure 11). **INT-1A** is the lowest energy non-hydridic complex, but it is not the resting state of the catalyst (vide infra), in agreement with the experimental results.

The catalytic cycle begins with formation of a hydrogen bond between benzyl alcohol **5a** and the alkoxide ligand of **INT-1**, forming **INT-2**. At this point, the outer- and inner-sphere pathways diverge but merge again later at the stage of the hydrogenated catalyst (**INT-9**) (Figure 12). From **INT-2**, the outer-sphere route involves a single step ($\mathbf{TS}_{2\text{-}9}$), in which the oxidation of **5a** occurs by concerted synchronous transfer of the α-hydrogen and the proton from the alcohol to the metal center and the tethered alkoxide, respectively, in a cyclic six-membered transition state. The overall barrier for the outer-sphere dehydrogenation is 69 kJ/mol relative to **INT-1A**.

The inner-sphere mechanism consists of several steps. The first step is the coordination of benzyl alcohol **5a** to iridium (**INT-3**), followed by a proton transfer from **5a** to the tethered alkoxide ($\mathbf{TS}_{3\text{-}4}$). Upon protonation, the tethered alcohol dissociates from iridium ($\mathbf{TS}_{4\text{-}5}$) to give **INT-5**. This complex, like **INT-1**, contains only three ligands, and the alkoxide shows strong π donation to iridium (Ir−O distance 1.97 Å). The calculations revealed that, for the subsequent β-hydride elimination to occur, **INT-5** must first undergo a rearrangement into intermediate **INT-6**, in which there is an agostic interaction between the metal center and one of the benzylic C−H bonds.[20,33] Formation of the agostic intermediate is facilitated by a hydrogen bond between the substrate alkoxide ligand and the hydroxyl group on the carbene ligand. This diminishes the π donation from the alkoxide to the iridium center, which results in a longer Ir−O distance (2.09 Å) for this intermediate. From **INT-6**, the inner-sphere β-hydride elimination ($\mathbf{TS}_{6\text{-}7}$) takes place with a negligible energy barrier of ∼1 kJ/mol. Hence, formation of **INT-6** represents the major contribution to the overall energy barrier in the alcohol oxidation via the inner-sphere mechanism (69 kJ/mol from **INT-1A** to $\mathbf{TS}_{6\text{-}7}$). **INT-7**, the product of the β-hydride elimination, contains a molecule of benzaldehyde π bonded to iridium. After a change in the coordination mode from π to σ bonding ($\mathbf{TS}_{7\text{-}8}$), the benzaldehyde is replaced by the tethered alcohol ($\mathbf{TS}_{8\text{-}9}$).

Overall, since the energy barriers for the inner- and outer-sphere mechanisms of the alcohol oxidation are calculated to be practically the same (69 kJ/mol relative to **INT-1A**), it can be concluded that both pathways might operate concurrently or that there is a small difference that cannot be ascertained by the current level of modeling.[27,34] For the inner-sphere mechanism, the highest-energy TS is seen for the formation of the agostic bond ($\mathbf{TS}_{5\text{-}6}$), with only a marginal elongation of the C−H bond whereas, in the outer-sphere mechanism, both the C−H and O−H bonds are elongated in the TS ($\mathbf{TS}_{2\text{-}9}$, Figure 13). Therefore, we would expect a strong KIE from the outer-sphere mechanism but not from the inner-sphere mechanism. The calculated KIEs (at 80 °C) for those steps were 3.3 and 1.7 for the outer- and inner-sphere mechanisms, respectively (see the Supporting Information for the details). The competition experiment (vide supra) gave a KIE of 2.42 ± 0.07, which, in combination with the computational results, suggests that both calculated mechanisms can contribute in the alcohol dehydrogenation step.

Formation of the Imine and the Iridium−Hydride−Aniline Complex. Aldehyde **9** dissociates from **INT-9**, giving iridium hydride **INT-10**. This is an endergonic process by 8 kJ/mol (Figure 12). The results of the experimental studies indicated that the aldehyde does dissociate. **INT-10** may coordinate a molecule of aniline (**6a**) to give **INT-10A** (Figure 14), whose calculated energy is lower than that of **INT-9**. Formation of an iridium−hydride complex with aniline coordinated was

DOI: 10.1021/acscatal.5b00645
ACS Catal. 2015, 5, 3704−3716

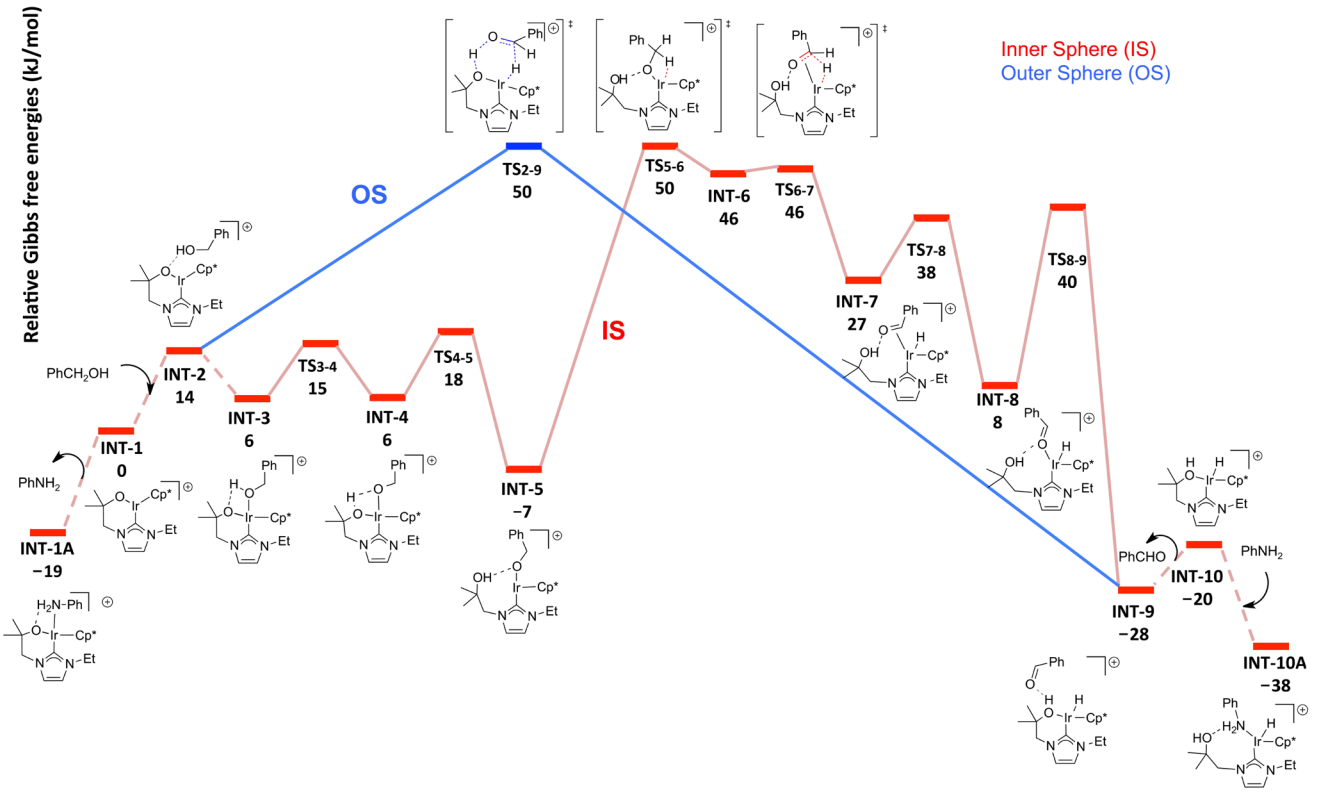

Figure 12. Calculated free-energy profile for the dehydrogenation of benzyl alcohol with the bifunctional iridium catalyst. All energies are given relative to **INT-1** + **5a** + **6a** in kJ/mol.

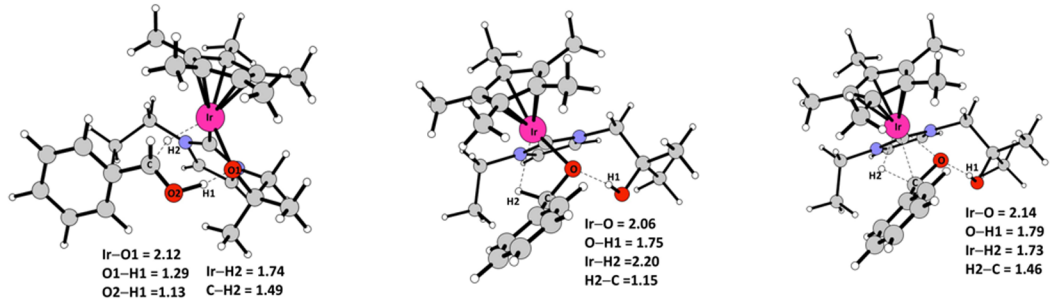

(a) **TS2-9** (50 kJ/mol) (b) **TS5-6** (50 kJ/mol) (c) **TS6-7** (46 kJ/mol)

Figure 13. Selected transition states for the alcohol oxidation via (a) outer-sphere and (b, c) inner-sphere mechanisms. Distances are given in Å.

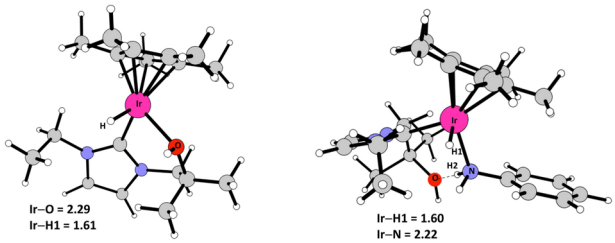

INT-10 (−11 kJ/mol) **INT-10A** (−29 kJ/mol)

Figure 14. Optimized structures of iridium hydride **INT-10** and resting state **INT-10A**. Distances are given in Å.

observed by ^{1}H NMR spectroscopy (vide supra), and it was suggested that this species is the resting state of the catalyst.[44]

The condensation between benzaldehyde (**9a**) and aniline (**6a**) was calculated to be endergonic by +9 kJ/mol (Figure 15).[45] There are a number of mechanistic possibilities for the imine formation, which can be mediated by either an iridium species[7c] or an anilinium salt (formed during the catalyst activation) acting as a Lewis or a Brønsted acid catalyst. These processes are expected to be rapid and reversible, and the mechanism, which includes acid−base equilibria and potentially zwitterionic intermediates, is not expected to be well modeled by standard DFT methods as employed here[34] and therefore were not studied explicitly beyond calculation of the thermodynamics of the overall imine formation. Assuming a rapid endergonic equilibrium (Curtin−Hammett conditions), the imine concentration (and therefore also the observed rate) will depend on the concentrations of all species in the equilibrium, in nice agreement with the observed inhibitory effect of water.

Imine Hydrogenation. For the hydrogenation of imine **8** to take place, **INT-10A** must first release the aniline ligand and subsequently bind imine **8** by hydrogen bonding to the tethered alcohol (Figure 15). From the resulting intermediate

DOI: 10.1021/acscatal.5b00645
ACS Catal. 2015, 5, 3704−3716

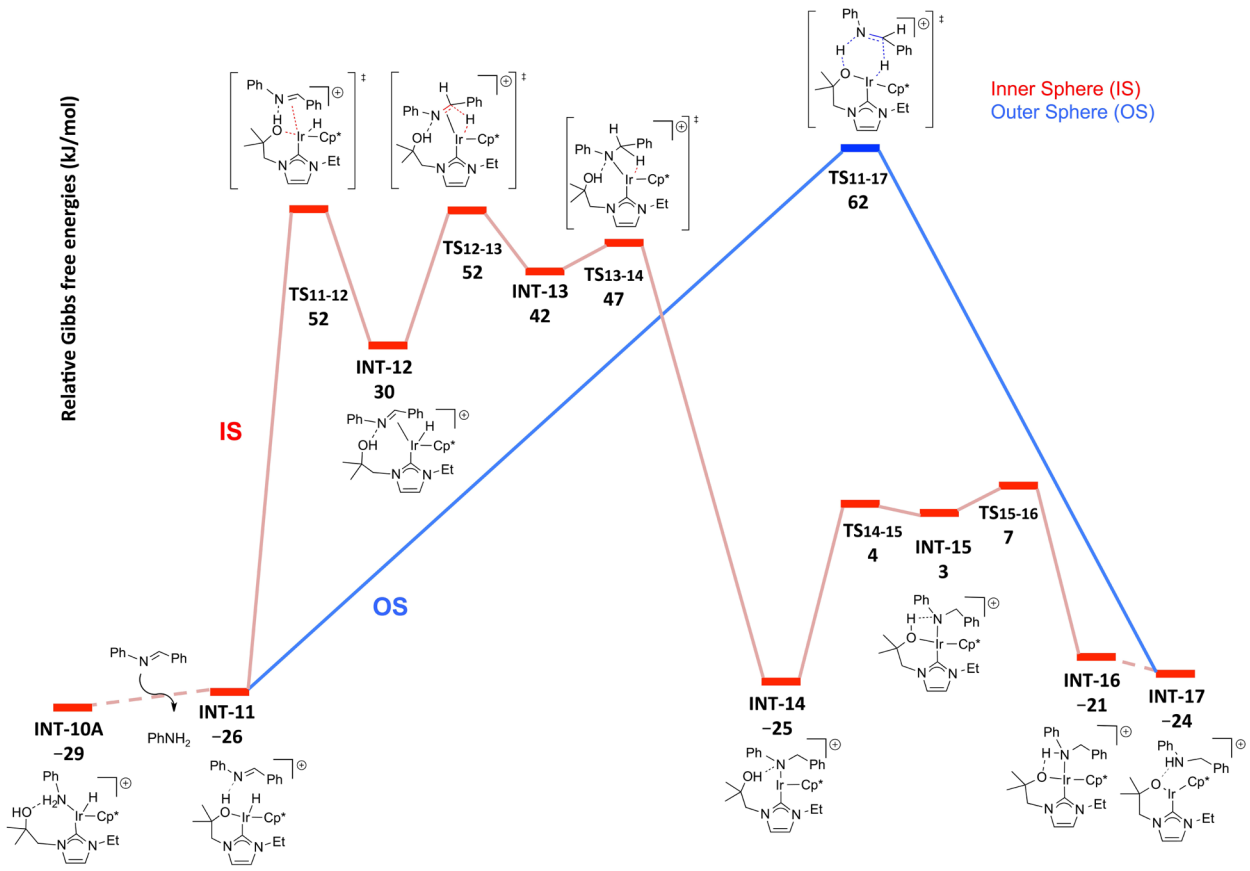

Figure 15. Calculated free-energy profile for hydrogenation of the imine with the bifunctional iridium catalyst. All energies are given relative to **INT-1** + **5a** + **6a**. Observe that the energy of **INT-10** (−11 kJ/mol) here includes the imine and therefore is 9 kJ/mol higher than that given in Figure 12.

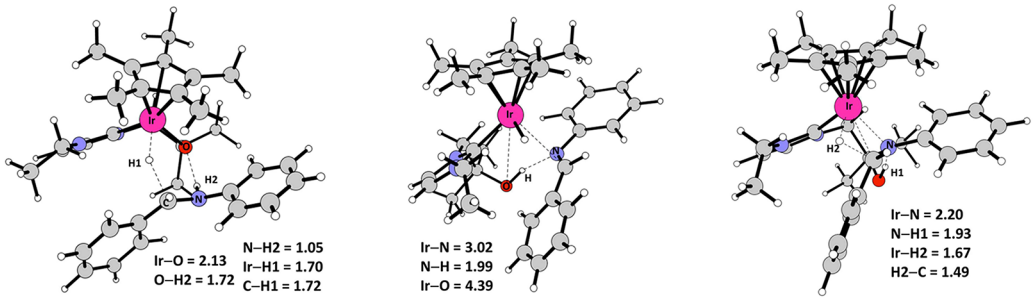

(a) $\mathbf{TS}_{11\text{-}17}$ (62 kJ/mol) (b) $\mathbf{TS}_{11\text{-}12}$ (52 kJ/mol) (c) $\mathbf{TS}_{12\text{-}13}$ (52 kJ/mol)

Figure 16. Transition states for imine hydrogenation via the (a) outer-sphere and (b, c) inner-sphere mechanisms. Distances are given in Å.

INT-11, the outer- and inner-sphere mechanisms diverge. Similarly to the alcohol oxidation, the former alternative involves only a single step leading directly to **INT-17**, which contains the final product (i.e., *sec*-amine **7**) hydrogen-bonded to the tethered alkoxide. The corresponding concerted transition state ($\mathbf{TS}_{11\text{-}17}$, Figure 16) is analogous to $\mathbf{TS}_{2\text{-}9}$, but in this case, proton and hydride are transferred asynchronously.[35] The overall barrier for this step is 91 kJ/mol (from **INT-10A** to $\mathbf{TS}_{11\text{-}17}$).

The inner-sphere route for the imine hydrogenation consists of steps similar to the reverse of the alcohol oxidation. Specifically, first the tethered alcohol decoordinates from iridium to allow complexation of the imine to the metal center through a π-bond ($\mathbf{TS}_{11-12}$, Figure 16).[46] From the resulting intermediate **INT-12**, the hydride addition (migratory insertion) occurs via $\mathbf{TS}_{12-13}$ (Figure 16). The addition is facilitated by an increased electrophilicity of the imine as a result of its coordination to iridium, as well as hydrogen bonding to the alcohol ligand.

$\mathbf{TS}_{12\text{-}13}$ leads to transient intermediate **INT-13**, which has an agostic interaction between the Ir center and an α-C–H bond of the amine. The transformation of **INT-13** into **INT-14**, in which the final reaction product is coordinated to iridium, is strongly exergonic. Similarly to **INT-5**, the electron-deficient metal center in **INT-14** is stabilized by π donation from the N of the amido ligand.[36] **INT-14** undergoes sequential coordination of the tethered alcohol to iridium ($\mathbf{TS}_{14\text{-}15}$), followed by proton transfer ($\mathbf{TS}_{15\text{-}16}$). Dissociation of the amine product from the iridium center forms **INT-17**, in which the amine product remains hydrogen bonded.

DOI: 10.1021/acscatal.5b00645
ACS Catal. 2015, 5, 3704−3716

Scheme 9. Mechanism for the Alkylation of Aniline with Benzyl Alcohol Catalyzed by Bifunctional Complex 1

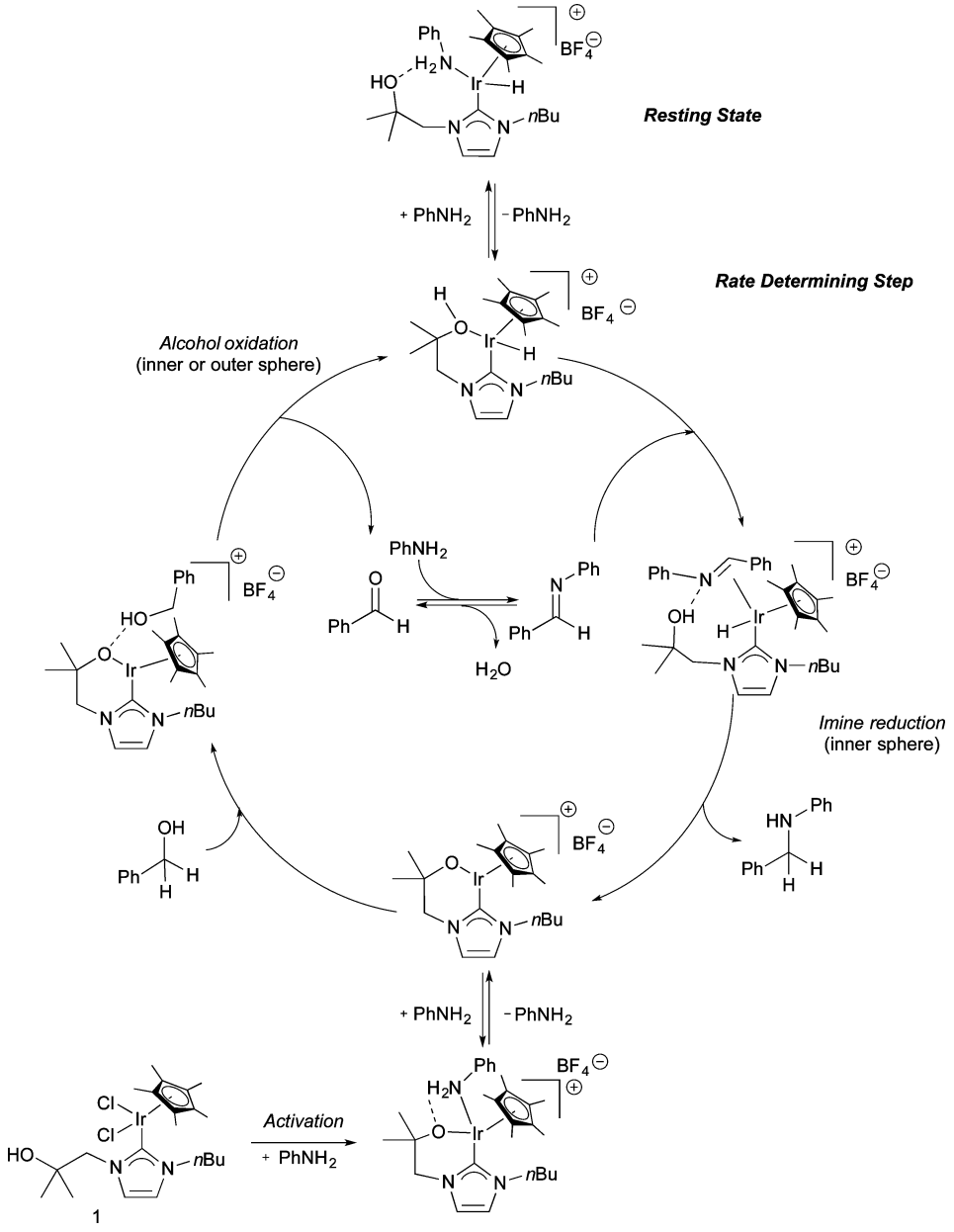

In contrast to the alcohol oxidation, in the last part of the mechanism (i.e., imine hydrogenation), the inner-sphere mechanism is clearly favored over the outer-sphere mechanism by 10 kJ/mol ($\mathbf{TS}_{11\text{-}12}$ or $\mathbf{TS}_{12\text{-}13}$ vs $\mathbf{TS}_{11\text{-}17}$) for the catalyst studied. This agrees well with our previous investigations showing that a related catalyst bearing an ether substituent on the carbene ligand was also able to afford good conversion; however the latter occurred under harsher reaction conditions with a higher catalyst loading.[12]

The calculated KIEs for the imine coordination step ($\mathbf{TS}_{11\text{-}12}$) and inner sphere hydride transfer from iridium to imine ($\mathbf{TS}_{12\text{-}13}$) are 1.0 and 1.6, respectively. The first value is closer to the experimental KIE of 1.24 ± 0.35, which further supports that imine coordination is the rds (see the Supporting Information for more details). The catalytic cycle is closed by the release of amine **7a** and the regeneration of **INT-1**. The overall reaction is exergonic by 21 kJ/mol.

Summary of the Theoretical Mechanistic Studies. It can be concluded that the alcohol oxidation step can occur by either an inner-sphere or an outer-sphere mechanism, which suggests that the electronic and steric properties of the particular substrate will determine which mechanism operates in each case. For the imine hydrogenation step the inner-sphere mechanism is favored, with a 10 kJ/mol difference in energy between the highest transition states for the outer-sphere ($\mathbf{TS}_{11\text{-}17}$) and inner-sphere ($\mathbf{TS}_{11\text{-}12}$ or $\mathbf{TS}_{12\text{-}13}$) pathways.

The highest energy span for the imine hydrogenation part of the mechanism (via the inner-sphere pathway) is located between **INT-10A** and $\mathbf{TS}_{11\text{-}12}$ (81 kJ/mol). It is higher than the overall barrier for the alcohol oxidation (69 kJ/mol), which is consistent with the experimental results, and indicates that the rds is located in the second part of the mechanism (imine reduction) and not in the alcohol oxidation part. **INT-10A** is thus identified as the resting state of the catalyst, and its structure correlates with that of aniline coordinated hydride **A1**

DOI: 10.1021/acscatal.5b00645
ACS Catal. 2015, 5, 3704−3716

proposed in the experimental investigations. The rds involves the dissociation of aniline from iridium−hydride complex **INT-10A** followed by coordination of imine **8**. This agrees well with the experimentally observed inhibiting effects of aniline (**6a**) and water and with the accelerating effect of added imine **8**. Transition state $\mathbf{TS}_{11\text{-}12}$ does not involve a hydrogen transfer, which is consistent with the experimentally observed low KIE in the reaction. Hydride transfer transition state $\mathbf{TS}_{12\text{-}13}$ is calculated to be isoergic with $\mathbf{TS}_{11\text{-}12}$, but in this case, the results of the Hammett studies show that the rate-limiting step is indeed coordination, $\mathbf{TS}_{11\text{-}12}$. The real energy difference between these two steps is simply too small to be captured accurately by the DFT methods used here.[34] The highest calculated energy for the alcohol dehydrogenation ($\mathbf{TS}_{2\text{-}9}$ and $\mathbf{TS}_{5\text{-}6}$ at 50 kJ/mol) is slightly lower than the highest calculated energy in the inner-sphere imine hydrogenation sequence ($\mathbf{TS}_{11\text{-}12}$ and $\mathbf{TS}_{12\text{-}13}$ at 52 kJ/mol. This should indicate that the former step is reversible. This contrasts with the experimental results obtained in the competition crossover experiment (Scheme 5), in which a very small amount of monodeuterated **5**-d_1 was produced, and also with the observed stereochemical integrity of chiral alcohol (*R*)-**10** (Scheme 6). However, it must be noted that all calculations deliver results at the standard state, 1 M solution of all participating species and that the reaction is run at infinite dilution in the solvent of choice. Imine formation, disfavored under standard conditions according to the calculated energies, is actually favored under real experimental reaction conditions, as was observed during the kinetic experiments. The concentration of aniline is higher than that of water, especially in the initial phase of reaction, shifting the equilibrium toward imine formation. Hence, on the basis of experimental studies, we can presume that the imine coordination step ($\mathbf{TS}_{11\text{-}12}$) is slightly lower in energy than the alcohol oxidation step ($\mathbf{TS}_{5\text{-}6}$ or $\mathbf{TS}_{2\text{-}9}$) in the initial phase of the reaction but becomes competitive eventually, when concentrations have shifted sufficiently to allow back-reaction to alcohol.

In addition, the theoretical investigations support the importance of the bifunctional character of the hydroxyl-functionalized carbene ligand and its participation throughout the catalytic cycle. This is in agreement with the greatly reduced activity observed when a related complex, in which the hydroxyl functionality had been replaced by a methyl ether group, was used.[12]

By combining the results from the experimental investigations with those obtained computationally, we propose the catalytic cycle depicted in Scheme 9.

CONCLUSIONS

The rate of the alkylation of aniline (**6a**) with benzyl alcohol (**5a**) catalyzed by iridium(III) complex **1** was established experimentally to be zero order with respect to benzyl alcohol (**5a**), second order in catalyst **1**, and negative first order in water and aniline (**6a**). The rate is also zero order with respect to the product of the reaction (benzylaniline **7a**). Furthermore, as supported by Hammett studies and kinetic isotope investigations, the coordination of the imine intermediate (**8**) to an iridium hydride species constitutes the rate-determining step of the reaction. The resting state is in the form of an iridium hydride with the aniline substrate coordinated, as observed by NMR spectroscopy. Further evidence suggesting a resting state formed upon coordination of the aniline substrate to iridium was obtained by one-pot Hammett competition studies. These conclusions were well supported computationally. In addition, the theoretical investigations also showed that the alcohol oxidation step follows either an outer- or an inner-sphere pathway, while the inner-sphere mechanism seems dominant for the reduction of the imine intermediate by the iridium hydride. We have also investigated the role of the alcohol-functionalized carbene ligand in complex **1** and showed that it participates in almost every step of the catalytic cycle by donating or accepting protons to or from the substrates, as well as by hydrogen bonding to substrates and intermediates, facilitating the reaction. Thus, the efficient catalytic behavior of complex **1** (i.e., additional base is not needed, an excess of any of the substrates is not required, and the reaction can proceed at mild temperatures, 50 °C)[12] can be ascribed to the presence of a bidentate and bifunctional nature of this unique iridium carbene complex **1**.

EXPERIMENTAL SECTION

General Considerations. All reactions were carried out under an argon atmosphere in oven-dried glassware. The sealable tubes used were Biotage microwave vials. Reagents were of analytical grade and were obtained from commercial suppliers and used as purchased. CH_2Cl_2 was dried over CaH_2 and distilled under nitrogen. Anhydrous toluene was obtained using a VAC solvent purifier system. ^1H and ^{13}C NMR spectra were recorded at 500 and 125 MHz, respectively, using a Bruker Avance spectrometer. Chemical shifts (δ) are reported in ppm, using the residual solvent peak in $CDCl_3$ (δ_H 7.26 ppm) as a reference. Enantiomeric excess was determined by HPLC analysis (Waters 2695).

Computational Details. Calculations were carried out using the Jaguar package.[37] Geometries were optimized using the B3LYP functional[38] with the LACVP* basis set.[39] These were then characterized with frequency calculations to confirm their character as minima (no imaginary frequencies) or transition states (a single imaginary frequency). The connections between transition states and their corresponding reactants and products were verified by fully optimizing structures derived from the transition states with a small displacement following the transition vector in both directions (QRC).[40] The final Gibbs free energies were obtained from single-point calculations using the M06 functional[41] with the larger basis set LACV3P**$^+$, corrected for zero-point and thermal effects at 353.0 K and 325.0 atm from the frequency calculations,[33b] and solvation free energies. The effect of the solvent was calculated using a self-consistent reaction field (SCRF) polarized continuum model (PBF) with parameters for benzene,[42] implemented in Jaguar.

ASSOCIATED CONTENT

Supporting Information

The Supporting Information is available free of charge on the ACS Publications website at DOI: 10.1021/acscatal.5b00645.

Procedures, full kinetic analysis, and further experimental details (PDF)

Cartesian coordinates and energies of the calculated geometries (PDF)

AUTHOR INFORMATION

Corresponding Author

*belen.martin.matute@su.se.

DOI: 10.1021/acscatal.5b00645
ACS Catal. 2015, 5, 3704−3716

Author Contributions

⊥A.B., G.G.M., and R.M. contributed equally.

Notes

The authors declare no competing financial interest.

■ ACKNOWLEDGMENTS

Financial support was obtained from the Swedish Research Council (VR), the Swedish Governmental Agency for Innovation Systems (VINNOVA) through the Berzelii Center EXSELENT, the Knut and Alice Wallenberg Foundation, and the Wenner-Gren Foundation. B.M.-M. also thanks VINNOVA for a VINNMER grant.

■ REFERENCES

(1) (a) Hamid, M. H. S. A.; Slatford, P. A.; Williams, J. M. J. *Adv. Synth. Catal.* **2007**, *349*, 1555−1575. (b) Nixon, T. D.; Whittlesey, M. K.; Williams, J. M. J. *Dalton Trans.* **2009**, *38*, 753−762. (c) Guillena, G.; Ramón, D. J.; Yus, M. *Chem. Rev.* **2010**, *110*, 1611−1641. (d) Dobereiner, G. E.; Crabtree, R. H. *Chem. Rev.* **2010**, *110*, 681−703. (e) Watson, A. J. A.; Williams, J. M. J. *Science* **2010**, *329*, 635−636. (f) Bähn, S.; Imm, S.; Neubert, L.; Zhang, M.; Neumann, H.; Beller, M. *ChemCatChem* **2011**, *3*, 1853−1864. (g) Pan, S.; Shibata, T. *ACS Catal.* **2013**, *3*, 704−712.

(2) (a) Müller, T. E.; Beller, M. *Chem. Rev.* **1998**, *98*, 675−703. (b) Müller, T. E.; Hultzsch, K. C.; Yus, M.; Foubelo, F.; Tada, M. *Chem. Rev.* **2008**, *108*, 3795−3892. (c) Nugent, T. C.; El-Shazly, M. *Adv. Synth. Catal.* **2010**, *352*, 753−819. (d) Krüger, K.; Tillack, A.; Beller, M. *ChemSusChem* **2009**, *2*, 715−717. (e) Ward, J.; Wohlgemuth, R. *Curr. Org. Chem.* **2010**, *14*, 1914−1927. (f) Crozet, D.; Urrutigoïty, M.; Kalck, P. *ChemCatChem* **2011**, *3*, 1102−1118. (g) Gunanathan, C.; Milstein, D. *Science* **2013**, *341*, 249−261. (h) Banerjee, D.; Junge, K.; Beller, M. *Angew. Chem.* **2014**, *126*, 13265−13269; *Angew. Chem., Int. Ed.* **2014**, *53*, 13049−13053.

(3) Early reports: (a) Watanabe, Y.; Tsuji, Y.; Ohsugi, Y. *Tetrahedron Lett.* **1981**, *22*, 2667−2670. (b) Grigg, R.; Mitchell, T. R. B.; Sutthivaiyakit, S.; Tongpenyai, N. *J. Chem. Soc., Chem. Commun.* **1981**, 611−612.

(4) (a) Yamaguchi, R.; Mingwen, Z.; Kawagoe, S.; Asai, C.; Fujita, K.-i. *Synthesis* **2009**, *7*, 1220−1223. (b) Kawahara, R.; Fujita, K.-i.; Yamaguchi, R. *J. Am. Chem. Soc.* **2010**, *132*, 15108−15111. (c) Kawahara, R.; Fujita, K.-i.; Yamaguchi, R. *Adv. Synth. Catal.* **2011**, *353*, 1161−1168.

(5) (a) Bähn, S.; Tillack, A.; Imm, S.; Mevius, K.; Michalik, D.; Hollmann, D.; Neubert, L.; Beller, M. *ChemSusChem* **2009**, *2*, 551−557. (b) Bähn, S.; Imm, S.; Mevius, K.; Neubert, L.; Tillack, A.; Williams, J. M. J.; Beller, M. *Chem. - Eur. J.* **2010**, *16*, 3590−3593. (c) Imm, S.; Bähn, S.; Zhang, M.; Neubert, L.; Neumann, H.; Klasovsky, F.; Pfeffer, J.; Haas, T.; Beller, M. *Angew. Chem.* **2011**, *123*, 7741−7745; *Angew. Chem., Int. Ed.* **2011**, *50*, 7599−7603. (d) Zhang, M.; Imm, S.; Bähn, S.; Neumann, H.; Beller, M. *Angew. Chem.* **2011**, *123*, 11393−11397; *Angew. Chem., Int. Ed.* **2011**, *50*, 11197−11201.

(6) (a) Blank, B.; Michlik, S.; Kempe, R. *Chem. - Eur. J.* **2009**, *15*, 3790−3799. (b) Blank, B.; Michlik, S.; Kempe, R. *Adv. Synth. Catal.* **2009**, *351*, 2903−2911. (c) Blank, B.; Kempe, R. *J. Am. Chem. Soc.* **2010**, *132*, 924−925. (d) Michlik, S.; Kempe, R. *Chem. - Eur. J.* **2010**, *16*, 13193−13198. (e) Michlik, S.; Hille, T.; Kempe, R. *Adv. Synth. Catal.* **2012**, *354*, 847−862. (f) Ruch, S.; Irrgang, T.; Kempe, R. *Chem. - Eur. J.* **2014**, *20*, 13279−13285.

(7) (a) Tursky, M.; Lorentz-Petersen, L. L. R.; Olsen, L. B.; Madsen, R. *Org. Biomol. Chem.* **2010**, *8*, 5576−5582. (b) Monrad, R. N.; Madsen, R. *Org. Biomol. Chem.* **2011**, *9*, 610−615. (c) Fristrup, P.; Tursky, M.; Madsen, R. *Org. Biomol. Chem.* **2012**, *10*, 2569−2577. (d) Lorentz-Petersen, L. L. R.; Nordstrøm, L. U.; Madsen, R. *Eur. J. Org. Chem.* **2012**, *34*, 6752−6759.

(8) (a) Martínez, R.; Ramón, D. J.; Yus, M. *Org. Biomol. Chem.* **2009**, *7*, 2176−2181. (b) Cano, R.; Ramón, D. J.; Yus, M. *J. Org. Chem.* **2011**, *76*, 5547−5557. (c) Martínez-Asencio, A.; Ramón, D. J.; Yus, M. *Tetrahedron* **2011**, *67*, 3140−3149. (d) Martínez-Asencio, A.; Yus, M.; Ramón, D. J. *Synthesis* **2011**, *22*, 3730−3740.

(9) (a) Prades, A.; Corberán, R.; Poyatos, M.; Peris, E. *Chem. - Eur. J.* **2008**, *14*, 11474−11479. (b) Segarra, C.; Mas-Marzá, E.; Mata, J. A.; Peris, E. *Adv. Synth. Catal.* **2011**, *353*, 2078−2084.

(10) For recent examples, see: (a) Li, J.-Q.; Andersson, P. G. *Chem. Commun.* **2013**, *49*, 6131−6133. (b) Wang, D.; Zhao, K.; Xu, C.; Miao, H.; Ding, Y. *ACS Catal.* **2014**, *4*, 3910−3918. (c) Enyong, A. B.; Moasser, B. *J. Org. Chem.* **2014**, *79*, 7553−7563. (d) Zhang, Y.; Lim, C.-S.; Sim, D. S. B.; Pan, H.-J.; Zhao, Y. *Angew. Chem.* **2014**, *126*, 1423−1427; *Angew. Chem., Int. Ed.* **2014**, *53*, 1399−1403. (e) Oldenhuis, N. J.; Dong, V. M.; Guan, Z. *J. Am. Chem. Soc.* **2014**, *136*, 12548−12551. (f) Yan, T.; Feringa, B. L.; Barta, K. *Nat. Commun.* **2014**, *5*, 5602. (g) Rawlings, A. J.; Diorazio, L. J.; Wills, M. *Org. Lett.* **2015**, *17*, 1086−1089.

(11) (a) Cumpstey, I.; Agrawal, S.; Borbas, E. K.; Martín-Matute, B. *Chem. Commun.* **2011**, *47*, 7827−7829. (b) Agrawal, S.; Lenormand, M.; Martín-Matute, B. *Org. Lett.* **2012**, *14*, 1456−1459.

(12) Bartoszewicz, A.; Marcos, R.; Sahoo, S.; Inge, A. K.; Zou, X.; Martín-Matute, B. *Chem. - Eur. J.* **2012**, *18*, 14510−14519.

(13) Selected reviews: (a) Muñiz, K. *Angew. Chem., Int. Ed.* **2005**, *44*, 6622−6627. (b) Ikariya, T.; Kuwata, S.; Kayaki, Y. *Pure Appl. Chem.* **2010**, *82*, 1471−1483.

(14) Gunanathan, C.; Milstein, D. *Acc. Chem. Res.* **2011**, *44*, 588−602.

(15) Selected examples: (a) Shvo, Y.; Czarkie, D.; Rahamim, Y.; Chodosh, D. F. J. *J. Am. Chem. Soc.* **1986**, *108*, 7400−7402. (b) M. J. Mays, M. J.; Morris, M. J.; Raithby, P. R.; Shvo, Y.; Czarkie, D. *Organometallics* **1989**, *8*, 1162−1167. (c) Casey, C. P.; Singer, S. W.; Powell, D. R.; Hayashi, R. K.; Kavana, M. *J. Am. Chem. Soc.* **2001**, *123*, 1090−1100. (d) Casey, C. P.; Johnson, J. B.; Singer, S. W.; Cui, Q. *J. Am. Chem. Soc.* **2005**, *127*, 3100−3109. (e) Yamaguchi, R.; Ikeda, C.; Takahashi, Y.; Fujita, K-i. *J. Am. Chem. Soc.* **2009**, *131*, 8410−8412. (f) Conley, B. L.; Pennington-Boggio, M. K.; Boz, E.; Williams, T. J. *Chem. Rev.* **2010**, *110*, 2294−2312. (g) Bauer, G.; Kirchner, A. K. *Angew. Chem.* **2011**, *123*, 5918−5920; *Angew. Chem., Int. Ed.* **2011**, *50*, 5798−5800.

(16) Noyori, R.; Yamakawa, M.; Hashiguchi, S. *J. Org. Chem.* **2001**, *66*, 7931−7944.

(17) Blum, Y.; Czarkie, D.; Rahamim, Y.; Shvo, Y. *Organometallics* **1985**, *4*, 1459−1461.

(18) For a pendant alkoxide/alkoxide group in the Pt-catalyzed hydration of nitriles, see; (a) Ghaffar, T.; Parkins, A. W. *Tetrahedron Lett.* **1995**, *36*, 8657−8660. (b) Ghaffar, T.; Parkins, A. W. *J. Mol. Catal. A: Chem.* **2000**, *160*, 249−261. (c) Jiang, X.-B.; Minnaard, A. J.; Feringa, B. L.; De Vries, J. G. *J. Org. Chem.* **2004**, *69*, 2327−2331. A catalyst that could be considered to be a metal−ligand bifunctional catalyst: (d) Peñafiel, I.; Pastor, I. M.; Yus, M.; Esteruelas, M. A.; Oliván, M. *Organometallics* **2012**, *31*, 6154−6161. Work suggesting potential use of tertiary alkoxides ligands in bifunctional catalysts: (e) Schley, N. D.; Halbert, S.; Raynaud, C.; Eisenstein, O.; Crabtree, R. H. *Inorg. Chem.* **2012**, *51*, 12313−12323.

(19) (a) Liu, C.; Liao, S.; Li, Q.; Feng, S.; Sun, Q.; Yu, X.; Xu, Q. *J. Org. Chem.* **2011**, *76*, 5759−5773. (b) Martínez-Asencio, A.; Ramón, D. J.; Yus, M. *Tetrahedron* **2011**, *67*, 3140−3149. (c) Li, Q.; Fan, S.; Sun, Q.; Tian, H.; Yu, X.; Xu, Q. *Org. Biomol. Chem.* **2012**, *10*, 2966−2972. (d) Zhao, Y.; Foo, S. W.; Saito, S. *Angew. Chem.* **2011**, *123*, 3062−3065; *Angew. Chem., Int. Ed.* **2011**, *50*, 3006−3009. (e) Zhang, Y.; Qi, X.; Cui, X.; Shi, F.; Deng, Y. *Tetrahedron Lett.* **2011**, *52*, 1334−1338. (f) Weickmann, D.; Frey, W.; Plietker, B. *Chem. - Eur. J.* **2013**, *19*, 2741−2748.

(20) Bacells, D.; Nova, A.; Clot, E.; Gnanamgari, D.; Crabtree, R. H.; Eisenstein, O. *Organometallics* **2008**, *27*, 2529−2535.

(21) For experimental and theoretical studies on transfer hydrogenation with other Ir systems: (a) Campos, J.; Hintermair, U.; Brewster, T. P.; Takase, M. K.; Crabtree, R. H. *ACS Catal.* **2014**, *4*, 973−985. (b) Fujita, K.-i.; Yoshida, T.; Imori, Y.; Yamaguchi, R. *Org. Lett.* **2011**, *13*, 2278−2281. (c) Li, H.; Lu, G.; Jiang, J.; Huang, F.; Wang, Z.-X. *Organometallics* **2011**, *30*, 2349−2363. (d) Albrecht, M.;

DOI: 10.1021/acscatal.5b00645
ACS Catal. 2015, 5, 3704−3716

Miecznikowski, J. R.; Samuel, A.; Faller, J. W.; Crabtree, R. H. *Organometallics* **2002**, *21*, 3596−3604. (e) Hanasaka, F.; Fujita, K.-i.; Yamaguchi, R. *Organometallics* **2005**, *24*, 3422−3433. (f) Pàmies, O.; Bäckvall, J.-E. *Chem. - Eur. J.* **2001**, *7*, 5052−5058.

(22) (a) Royo, B.; Peris, E. *Eur. J. Inorg. Chem.* **2012**, *9*, 1309−1318. (b) da Costa, A. P.; Viciano, M.; Sanaú, M.; Merino, S.; Tejeda, J.; Peris, E.; Royo, B. *Organometallics* **2008**, *27*, 1305−1309. (c) Liu, C.; Liao, S.; Li, Q.; Feng, S.; Sun, Q.; Yu, X.; Xu, Q. *J. Org. Chem.* **2011**, *76*, 5759−5773. (d) Mehta, A.; Thaker, A.; Londhe, V.; Nandan, S. R. *Appl. Catal., A* **2014**, *478*, 241−251. (e) Satyanarayana, P.; Reddy, G. M.; Maheswaran, H.; Kantam, M. L. *Adv. Synth. Catal.* **2013**, *355*, 1859−1867.

(23) (a) Bullock, R. M. *Chem. - Eur. J.* **2004**, *10*, 2366−2374. (b) Samec, J. S. M.; Backvall, J.-E.; Andersson, P. G.; Brandt, P. *Chem. Soc. Rev.* **2006**, *35*, 237−248.

(24) (a) Samec, J. S. M.; Éll, A. H.; Åberg, J. B.; Privalov, T.; Eriksson, L.; Bäckvall, J.-E. *J. Am. Chem. Soc.* **2006**, *128*, 14293−14305. (b) Clapham, S. E.; Hadzovic, A.; Morris, R. H. *Coord. Chem. Rev.* **2004**, *248*, 2201−2237. (c) Casey, C. P.; Johnson, J. B. *J. Am. Chem. Soc.* **2005**, *127*, 1883−1894. (d) Casey, C. P.; Bikzhanova, G. A.; Cui, Q.; Guzei, I. A. *J. Am. Chem. Soc.* **2005**, *127*, 14062−14071. (e) Casey, C. P.; Johnson, J. B. *Can. J. Chem.* **2005**, *83*, 1339−1346. (f) Noyori, R.; Hashiguchi, S. *Acc. Chem. Res.* **1997**, *30*, 97−102. (g) Dorta, R.; Broggini, D.; Kissner, R.; Togni, A. *Chem. - Eur. J.* **2004**, *10*, 4546−4555.

(25) Feng, Y.; Jiang, B.; Boyle, P. A.; Ison, E. A. *Organometallics* **2010**, *29*, 2857−2867. (b) Neubert, L.; Michalik, D.; Bähn, S.; Imm, S.; Neumann, H.; Atzrodt, J.; Derdau, V.; Holla, W.; Beller, M. *J. Am. Chem. Soc.* **2012**, *134*, 12239−12244.

(26) Simmons, E. M.; Hartwig, J. F. *Angew. Chem., Int. Ed.* **2012**, *51*, 3066−3072.

(27) General perspective: Synergy between experiment and theory: Lupp, D.; Christensen, N. J.; Fristrup, P. *Dalton Transactions* **2014**, *43*, 11093−11105.

(28) (a) Hammett, L. P. *J. Am. Chem. Soc.* **1937**, *59*, 96−103. (b) Ingold, C. K.; Shaw, F. R. *J. Chem. Soc.* **1927**, 2918−2926.

(29) For 'one pot' Hammett investigations of stoichiometric reactions, see: Yau, H. M.; Croft, A. K.; Harper, J. B. *Chem. Commun.* **2012**, *48*, 8937−8939.

(30) For examples of other competition Hammett investigations of catalytic reactions, see: (a) Desai, L. V.; Strowers, K. J.; Sanford, M. S. *J. Am. Chem. Soc.* **2008**, *130*, 13285−13293. (b) Fristrup, P.; Kreis, M.; Palmelund, A.; Norrby, P.-O.; Madsen, R. *J. Am. Chem. Soc.* **2008**, *130*, 5206−5215. (c) Keinicke, L.; Fristrup, P.; Norrby, P.-O.; Madsen, R. *J. Am. Chem. Soc.* **2005**, *127*, 15756−15761. (d) Hedström, A.; Bollmann, U.; Bravidor, J.; Norrby, P.-O. *Chem. - Eur. J.* **2011**, *17*, 11991−11993.

(31) Curtin, D. Y. *Rec. Chem. Prog.* **1954**, *15*, 111−128.

(32) For Ir−alkoxide complexes, see ref 18e. Ru−alkoxide complexes: (a) Johnson, T. J.; Huffman, J. C.; Caulton, K. G. *J. Am. Chem. Soc.* **1992**, *114*, 2725−2727. (b) Caulton, K. G. *New J. Chem.* **1994**, *18*, 25−41. (c) Johnson, T. J.; Folting, K.; Streib, W. E.; Martin, J. D.; Huffman, J. C.; Jackson, S. A.; Eisenstein, O.; Caulton, K. G. *Inorg. Chem.* **1995**, *34*, 488−499. (d) Stewart, B.; Nyhlén, J.; Martín-Matute, B.; Bäckvall, J.-E.; Privalov, T. *Dalton Trans.* **2013**, *42*, 927−934.

(33) (a) Makarov, I. S.; Fristrup, P.; Madsen, R. *Chem. - Eur. J.* **2012**, *18*, 15683−15692. (b) Sieffert, N.; Bühl, M. *J. Am. Chem. Soc.* **2010**, *132*, 8056−8070.

(34) Plata, R. E.; Singleton, D. A. *J. Am. Chem. Soc.* **2015**, *137*, 3811−3826.

(35) (a) Chen, Y.; Liu, S.; Lei, M. *J. Phys. Chem. C* **2008**, *112*, 13524−13527. (b) Zhang, X.; Guo, X.; Chen, Y.; Tang, Y.; Lei, M.; Fang, W. *Phys. Chem. Chem. Phys.* **2012**, *14*, 6003−6012.

(36) (a) Glueck, D. S.; Wu, J. X.; Hollander, F. J.; Bergman, R. G. *J. Am. Chem. Soc.* **1991**, *113*, 2041−2054. (b) Macgregor, S. A.; Vadivelu, P. *Organometallics* **2007**, *26*, 3651−3659.

(37) *Jaguar, version 7.8*; Schrödinger, LLC, New York, 2011.

(38) (a) Becke, A. D. *J. Chem. Phys.* **1993**, *98*, 5648−5652. (b) Becke, A. D. *J. Chem. Phys.* **1993**, *98*, 1372−1377. (c) Lee, C.; Yang, W.; Parr, R. G. *Phys. Rev. B: Condens. Matter Mater. Phys.* **1988**, *37*, 785−789.

(39) LACVP* uses the 6-31G* basis set for all light elements and the Hay−Wadt ECP and basis set for Ir, see: Hay, P. J.; Wadt, W. R. *J. Chem. Phys.* **1985**, *82*, 299−310.

(40) Goodman, J. M.; Silva, M. A. *Tetrahedron Lett.* **2003**, *44*, 8233−8236.

(41) (a) Zhao, Y.; Truhlar, D. G. *Theor. Chem. Acc.* **2008**, *120*, 215−241. (b) Zhao, Y.; Truhlar, D. G. *Acc. Chem. Res.* **2008**, *41*, 157−167.

(42) (a) Tannor, D. J.; Marten, B.; Murphy, R.; Friesner, R. A.; Sitkoff, D.; Nicholls, A.; Ringnalda, M.; Goddard, W. A., III; Honig, B. *J. Am. Chem. Soc.* **1994**, *116*, 11875−11882. (b) Marten, B.; Kim, K.; Cortis, C.; Friesner, R. A.; Murphy, R. B.; Ringnalda, M. N.; Sitkoff, D.; Honig, B. *J. Phys. Chem.* **1996**, *100*, 11775−11788.

(43) With $[Cp^*IrCl_2]_2$ as the catalyst, inhibition by the aniline substrate was attributed to disfavored coordination of the alcohol substrate, rather than disfavored coordination of the imine intermediate. It was also shown that this inhibition is dependent on the structure of the amine substrate and/or product.[20]

(44) The coordination of **7a** to **INT-10** was also studied. The resulting complex, **INT-10B**, was found to have an energy similar to that of **INT-10** (−21 kJ/mol relative to **INT-1**). Hence, the binding of **7a** to the iridium hydride is much weaker than that of **6a**, which agrees well with the experimental findings.

(45) 9 kJ/mol refers to the formation of an (*E*)-imine. The formation of the corresponding (*Z*)-imine was also evaluated, but it was found to be higher in energy. Importantly, both isomers of the imine were tested in the subsequent hydrogenation step (via both the inner- and outer-sphere mechanisms), and the calculated energies for transition states involving the (*E*)-imine were uniformly lower. Therefore, the involvement of the (*Z*)-imine was ruled out.

(46) An alternative pathway from **INT-11** to **INT-12** via **INT-11A**, which contains a σ-bonded imine, was calculated. Relative Gibbs free energies of 42, 4, and 67 kJ/mol were found for $\mathbf{TS_{11\text{-}11A}}$, **INT-11A**, and $\mathbf{TS_{11A\text{-}12}}$, respectively. The TS energy was 42 kJ/mol.

DOI: 10.1021/acscatal.5b00645
ACS Catal. 2015, 5, 3704−3716